Soil Dynamics and Earthquake Engineering 196 (2025) 109437

Contents lists available at ScienceDirect

Soil Dynamics and Earthquake Engineering

journal homepage: www.elsevier.com/locate/soildyn

# Estimation of modal parameters of structures subjected to known base accelerations: Application to shake table tests

Javier Cara [a],*, David Escolano-Margarit [b], Amadeo Benavent-Climent [a]

[a] ETSI Industriales, Universidad Politécnica de Madrid, Spain
[b] Departamento de Mecánica de Estructuras e Ingeniería Hidráulica, Universidad de Granada, Spain

ARTICLE INFO

*Keywords:*
Operational Modal Analysis
Experimental Modal analysis
State space model
EM algorithm
Shaking table test

ABSTRACT

This paper presents a state space model along with a maximum likelihood algorithm to extract the modal parameters of structures when the vibrations are caused by ground accelerations and these accelerations are recorded. Shake table tests are well-known examples of these situations, but not the only ones. It is shown that in these cases the state space model used to compute the modal parameters is different from the conventional input–output model. Moreover, the proposed model consists of a set of equations that are the same regardless of whether absolute accelerations or relative displacements are used as output data. This is especially important in shake table tests because it is common to use different type of sensors, so it is suggested to exploit the above-mentioned fact to assess the consistency and reliability of the measurements obtained from different instruments (i.e. accelerometers and displacement transducers). The proposed model is estimated using the EM algorithm because the estimates are unbiased and with minimum variance. But the great advantage of this approach is that the EM algorithm can be adapted to estimate different models, in particular the one developed in this work. Finally, the proposed method (model and estimation algorithm) is applied to the experimental data measured during the shake table tests conducted on a reinforced concrete structure.

## 1. Introduction

Two main approaches can be found in the literature to extract the modal parameters of vibrating systems [1]. The first one is modal analysis using only output data, in which the forces causing the vibration of the structure are not used in the analysis (usually because they are not available) and the modal parameters are estimated using only the dynamic output response of the structure. This method is known as Operational Modal Analysis (OMA) and is the main modal testing method for large structures such as bridges [2], footbridges [3], high-rise buildings [4] or dams [5]. The second approach is the modal analysis using input and output data. In this case, some of the forces that cause the vibrations of the structure are measured and the modal parameters are computed from input and output measurements [6]. This method is usually known as Experimental Modal Analysis (EMA).

OMA and EMA can be performed using parametric and non-parametric methods. The parametric approach always involves two steps: (i) fitting a model to the data, and (ii) computing the modal parameters from this model. For the former, the state space model is the preferred option [1]. This model has different versions, depending on the type of data. For the analysis of output-only data (OMA), the state space model is given by Eqs. (1) and (2):

$$\mathbf{x}_{k+1} = \mathbf{A}\mathbf{x}_k + \mathbf{w}_k, \tag{1}$$

$$\mathbf{y}_k = \mathbf{C}\mathbf{x}_k + \mathbf{v}_k. \tag{2}$$

where $\mathbf{y}_k$ is the system output, $\mathbf{x}_k$ is an internal variable of the system, $\mathbf{A}$ and $\mathbf{C}$ are the state and output matrices, respectively; and $\mathbf{w}_k$ and $\mathbf{v}_k$ are random processes modeling the system and sensor errors. Since this model does not include the input of the structure, this input is considered as part of the noise variables.

The state space model for input–output data (EMA) is given by Eqs. (3) and (4):

$$\mathbf{x}_{k+1} = \mathbf{A}\mathbf{x}_k + \mathbf{B}\mathbf{u}_k + \mathbf{w}_k, \tag{3}$$

$$\mathbf{y}_k = \mathbf{C}\mathbf{x}_k + \mathbf{D}\mathbf{u}_k + \mathbf{v}_k. \tag{4}$$

where $\mathbf{y}_k$ is the measured output of the system and $\mathbf{u}_k$ is the measured system input; $\mathbf{B}$ and $\mathbf{D}$ are the input matrices. This model must be used when the (known) external force is applied directly to the structure. These forces are commonly generated by an impact hammer where the input force is recorded with a load cell attached to the striking face [7], or by a shaker that applies a forced excitation and is equipped with a load cell that measures magnitude and phase [6], or even using other types of actuators [8].

A similar situation arises when the vibration of the structure is induced by accelerations applied at the base of the system and this

* Corresponding author.
*E-mail address:* javier.cara@upm.es (J. Cara).

https://doi.org/10.1016/j.soildyn.2025.109437
Received 8 August 2024; Received in revised form 17 February 2025; Accepted 3 April 2025
Available online 19 April 2025

acceleration is recorded [9], although the best known example is the case of shake table tests. There are many examples of modal analysis using data recorded in a shake table test: for example, in [10] the modal parameters were evaluated by single-input-four-output ARX models and the least squares estimation; [11] used the deterministic subspace algorithm to estimate the modal parameters of a wind turbine under parked and operational conditions; in [12] the seismic performance of an existing masonry building with flexible floors was analyzed through several seismic tests with increasing amplitude. However, there are no details about the estimation method; [13] evaluated the effectiveness of automated modal parameter monitoring for vibration-based Structural Health Monitoring of existing bridges in seismic areas using shaking table tests. They applied OMA methods to estimate the modal parameters; in [14] a series of full-scale tests were conducted on a shaking table in Japan to simulate various levels of realistic seismic damage in a high-rise structural steel building using the frequency response function curve-fitting method and auto-regressive with exogenous term method; in [15] the continuous wavelet transform was used to investigate the change of modal frequencies before and after the structural damage; [16] presented a time-varying model-based method for estimating earthquake-induced displacement responses of building structures using the unscented Kalman filter; in [17] shake table testing was used for damage sensitivity of nonstructural elements in a fixed-base and a base-isolated building.

At first one might think that the state space model we have to use in the case of recorded base accelerations is model (3) and (4) since the system input and the output are known. However, a detailed analysis of the equations shows that the state space model for this particular case is given by the Eqs. (25) and (26). The main difference between both state space models is that the term **D** disappears, so the only way the ground accelerations are included in the model is by mean of the input matrix **B**. Therefore, the identification algorithms must be adapted according to the new model.

In this context, the objectives of this research are:

- The first one is to develop the equations of the state space model for a structure that is vibrating due to an excitation (*i.e.* a history of accelerations) applied at the base and these accelerations are recorded. As commented previously, the state space model given by Eqs. (3) and (4) does not include the base acceleration in the correct way. On the other hand, using the model given by Eqs. (1) and (2), that is, the OMA approach, is not optimum since the known base acceleration is not included in the analysis.
- The second objective is to propose an algorithm to estimate the proposed state space model. This is especially important because the modal parameters are computed from the estimated model. In this sense, the Expectation Maximization (EM) algorithm is proposed for this particular state space model. This is a maximum likelihood method, so in theory, estimates are unbiased and with minimum variance [18]. Although these properties make this algorithm a good choice, the main advantage is that it can be adapted to specific models, such as the one proposed in this work.
- The third objective is to use the proposed state space model and estimation method to obtain the modal parameters of a reinforced concrete structure tested under seismic loads on a shake table. The specimen considered in this work was instrumented with piezoelectric accelerometers that measured the absolute acceleration and displacement transducers (LVDTs) that measured the inter-story relative displacements at each level. Using different types of sensors is usual in this type of analysis, and it is shown that the proposed state space model is valid regardless of whether absolute accelerations or relative displacements are used as output data. This fact can be exploited to assess the accuracy, consistency and reliability of the measurements provided independently by the accelerometers and by the displacement transducers during shake table tests.

## 2. Proposed state space model for structures excited by a history of acceleration applied at the base

The dynamic behavior of a structure subjected to a ground motion can be represented by the second order differential equation [19]

$$\mathbf{M}\ddot{\mathbf{u}}(t) + \mathbf{G}\dot{\mathbf{q}}(t) + \mathbf{K}\mathbf{q}(t) = \mathbf{0}, \tag{5}$$

where

- $\mathbf{u}(t) \in \mathrm{R}^{n_d}$ is a vector containing the absolute displacements of $n_d$ selected points of the structure (the dot stands for the derivative with respect to the time);
- $\mathbf{q}(t)$ is the vector of relative displacements:

$$\mathbf{q}(t) = \mathbf{u}(t) - \mathbf{J}\mathbf{u}_g(t) \tag{6}$$

- $\mathbf{u}_g(t)$ is the vector with the components of the ground motion;
- $\mathbf{J} \in \mathbb{R}^{n_d \times 2}$ is a matrix with zeros and ones;
- $\mathbf{M} \in \mathbb{R}^{n_d \times n_d}$ is the mass matrix;
- $\mathbf{K} \in \mathbb{R}^{n_d \times n_d}$ is the stiffness matrix;
- $\mathbf{G} \in \mathbb{R}^{n_d \times n_d}$ is the damping matrix;

If we substitute Eq. (6) into (5) we have

$$\mathbf{M}\ddot{\mathbf{q}}(t) + \mathbf{G}\dot{\mathbf{q}}(t) + \mathbf{K}\mathbf{q}(t) = -\mathbf{M}\mathbf{J}\mathbf{a}(t),$$

$$\ddot{\mathbf{q}}(t) + \mathbf{M}^{-1}\mathbf{G}\dot{\mathbf{q}}(t) + \mathbf{M}^{-1}\mathbf{K}\mathbf{q}(t) = -\mathbf{J}\mathbf{a}(t), \tag{7}$$

where, for convenience, we have used $\mathbf{a}(t) = \ddot{\mathbf{u}}_g(t)$. Taking into account Eq. (7) and the trivial equation $\dot{\mathbf{q}}(t) = \dot{\mathbf{q}}(t)$, we can write

$$\begin{bmatrix}\dot{\mathbf{q}}(t)\\ \ddot{\mathbf{q}}(t)\end{bmatrix} = \begin{bmatrix}\mathbf{0} & \mathbf{I}\\ -\mathbf{M}^{-1}\mathbf{K} & -\mathbf{M}^{-1}\mathbf{G}\end{bmatrix}\begin{bmatrix}\mathbf{q}(t)\\ \dot{\mathbf{q}}(t)\end{bmatrix} + \begin{bmatrix}\mathbf{0}\\ -\mathbf{J}\end{bmatrix}\mathbf{a}(t) \tag{8}$$

This is a state equation in continuous time:

$$\dot{\mathbf{z}}(t) = \mathbf{A}_c\mathbf{z}(t) + \mathbf{B}_c\mathbf{a}(t) \tag{9}$$

where

$$\mathbf{z}(t) = \begin{bmatrix}\mathbf{q}(t)\\ \dot{\mathbf{q}}(t)\end{bmatrix}, \quad \mathbf{A}_c = \begin{bmatrix}\mathbf{0} & \mathbf{I}\\ -\mathbf{M}^{-1}\mathbf{K} & -\mathbf{M}^{-1}\mathbf{G}\end{bmatrix}, \quad \mathbf{B}_c = \begin{bmatrix}\mathbf{0}\\ -\mathbf{J}\end{bmatrix}. \tag{10}$$

When we work with absolute accelerations (for example, recorded using accelerometers), from Eq. (5):

$$\ddot{\mathbf{u}}(t) = \begin{bmatrix}-\mathbf{M}^{-1}\mathbf{K} & -\mathbf{M}^{-1}\mathbf{G}\end{bmatrix}\begin{bmatrix}\mathbf{q}(t)\\ \dot{\mathbf{q}}(t)\end{bmatrix} \Rightarrow \tag{11}$$

$$\ddot{\mathbf{u}}(t) = \mathbf{C}_{c1}\mathbf{z}(t) \tag{12}$$

where

$$\mathbf{C}_{c1} = \begin{bmatrix}-\mathbf{M}^{-1}\mathbf{K} & -\mathbf{M}^{-1}\mathbf{G}\end{bmatrix}. \tag{13}$$

Eqs. (9) and (12) define a state space model in continuous time.

In shake table test, it is also common to work with relative displacements recorded, for example, using LVDT or laser sensors. In these cases, we can write:

$$\mathbf{q}(t) = \begin{bmatrix}\mathbf{I} & \mathbf{0}\end{bmatrix}\begin{bmatrix}\mathbf{q}(t)\\ \dot{\mathbf{q}}(t)\end{bmatrix} \Rightarrow \tag{14}$$

$$\mathbf{q}(t) = \mathbf{C}_{c2}\mathbf{z}(t), \tag{15}$$

where

$$\mathbf{C}_{c2} = \begin{bmatrix}\mathbf{I} & \mathbf{0}\end{bmatrix}. \tag{16}$$

Eqs. (9) and (15) also define a state space model in continuous time but now expressed in terms of relative displacements. Whether relative displacements or absolute accelerations are used, the state space model can be written in general form as follows:

$$\dot{\mathbf{z}}(t) = \mathbf{A}_c\mathbf{z}(t) + \mathbf{B}_c\mathbf{a}(t), \tag{17}$$

$$\mathbf{y}(t) = \mathbf{C}_c \mathbf{z}(t), \tag{18}$$

where $\mathbf{y}(t) = \ddot{\mathbf{u}}(t)$, $\mathbf{C}_c = \mathbf{C}_{c1}$ if absolute accelerations are used; and $\mathbf{y}(t) = \mathbf{q}(t)$, $\mathbf{C}_c = \mathbf{C}_{c2}$ if relative displacements are employed. Since sensors record data in discrete time, it is necessary to convert the continuous time expressions into discrete time expressions. Using the constant approximation $\mathbf{a}(t_k) = \mathbf{a}_k,\ \forall t \in [t_k, t_k + \Delta t)$, we obtain (see [20]):

$$\mathbf{z}_{k+1} = \mathbf{A}_d \mathbf{z}_k + \mathbf{B}_d \mathbf{a}_k, \tag{19}$$

$$\mathbf{y}_k = \mathbf{C}_d \mathbf{z}_k, \tag{20}$$

where

$$\mathbf{z}_k = \begin{bmatrix} \mathbf{q}_k \\ \dot{\mathbf{q}}_k \end{bmatrix},\ \mathbf{A}_d = \exp\left(\mathbf{A}_c \Delta t\right),\ \mathbf{B}_d = (\mathbf{A}_d - \mathbf{I})\mathbf{A}_c^{-1}\mathbf{B}_c,\ \mathbf{C}_d = \mathbf{C}_c. \tag{21}$$

In data-driven modal analysis it is necessary to complete these equations with two random variables, $\mathbf{e}_k$ and $\mathbf{v}_k$, to take into account modeling errors and sensors noise. Thus, model (19)–(20) becomes

$$\mathbf{z}_{k+1} = \mathbf{A}_d \mathbf{z}_k + \mathbf{B}_d \mathbf{a}_k + \mathbf{e}_k, \tag{22}$$

$$\mathbf{y}_k = \mathbf{C}_d \mathbf{z}_k + \mathbf{v}_k, \tag{23}$$

In this work, we assume that these random variables follow a normal distribution:

$$\mathbf{e}_k \sim N(\mathbf{0}, \mathbf{Q}_d), \quad \mathbf{v}_k \sim N(\mathbf{0}, \mathbf{R}). \tag{24}$$

Finally, we must note that the state space model for a structure is not unique. In fact, we can use a generic state vector $\mathbf{x}_k$ such as $\mathbf{z}_k = \mathbf{T}\mathbf{x}_k$, where $\mathbf{T} \in \mathbb{R}^{2n_d \times 2n_d}$ is any non-singular matrix. Then, the state space model (22)–(23) becomes

$$\mathbf{x}_{k+1} = \mathbf{A}\mathbf{x}_k + \mathbf{B}\mathbf{a}_k + \mathbf{w}_k, \tag{25}$$

$$\mathbf{y}_k = \mathbf{C}\mathbf{x}_k + \mathbf{v}_k, \tag{26}$$

$$\mathbf{w}_k \sim N(\mathbf{0}, \mathbf{Q}),\ \mathbf{v}_k \sim N(\mathbf{0}, \mathbf{R}) \tag{27}$$

where

$$\mathbf{A} = \mathbf{T}^{-1}\mathbf{A}_d\mathbf{T}, \quad \mathbf{B} = \mathbf{T}^{-1}\mathbf{B}_d, \quad \mathbf{C} = \mathbf{C}_d\mathbf{T}, \quad \mathbf{Q} = \mathbf{T}^{-1}\mathbf{Q}_d\mathbf{T}. \tag{28}$$

In fact this is the model we estimate from the recorded data because the matrix $\mathbf{T}$ is unknown. The connection between the modal parameters and model (25)–(26) is given by the following property (see [20]):

**Property 2.1.** *The eigenvalues of matrix* $\mathbf{A}$ *are given by :*

$$\lambda_{2j-1,2j} = \exp\left[\left(-\zeta_j\omega_j \pm i\omega_j\sqrt{1-\zeta_j^2}\right)\Delta t\right],\ j = 1, 2, \ldots, n_d. \tag{29}$$

Therefore, the natural frequencies $\omega_j$ and the damping ratios $\zeta_j$ are given by

$$\omega_j = \frac{\left|\ln(\lambda_j)\right|}{\Delta t}, \tag{30}$$

$$\zeta_j = \frac{-\text{Real}\left[\ln(\lambda_j)\right]}{\omega_j \Delta t}. \tag{31}$$

On the other hand, the $jth$ mode shape $\boldsymbol{\phi}_j \in \mathbb{R}^{n_y}$ evaluated at sensor locations can be obtained using the following expression (see [20]):

$$\boldsymbol{\phi}_j = \mathbf{C}\boldsymbol{\psi}_j, \tag{32}$$

where $\boldsymbol{\psi}_j$ is the complex eigenvector of $\mathbf{A}$ corresponding to the eigenvalue $\lambda_j$.

Finally, the estimation of modal parameters can be summarized as follows:

- First, estimate the state space model (25)–(26) from the recorded data $\{\mathbf{y}_1, \mathbf{y}_2, \ldots, \mathbf{y}_N\}$ and $\{\mathbf{a}_1, \mathbf{a}_2, \ldots, \mathbf{a}_N\}$.
- Then, compute the modal parameters from the estimated model using Eqs. (30), (31) and (32).

The most critical point in this procedure is the estimation of the state space model. In the context of data-driven modal analysis, two main approaches can be found in the technical literature to estimate the state space model in the time domain:

- Subspace algorithms: This is perhaps the most used approach in Operational Modal Analysis (state space model (1)–(2)). We can find data-driven subspace algorithms and covariance-driven subspace algorithms [1]: they are based on least-squares estimation, so they are non-iterative algorithms; the results are, in general, unbiased and accurate. But, in contrast, it is more difficult to adapt the algorithm to specific problems.
- Maximum likelihood estimation using the EM algorithm: it is an iterative algorithm, so the estimation time is greater than the time needed for the subspace algorithms. According to the properties of maximum likelihood, the estimates should be unbiased and with minimum variance. But the great advantage of this approach is that the EM algorithm is highly adaptable to different models, and in particular, it can be formulated to estimate the model (25)–(26). That is the main reason we chose this algorithm in this work. The full approach is developed in the next Section.

## 3. The proposed estimation algorithm

### 3.1. Maximum likelihood estimation

Maximum likelihood is a method for estimating the parameters of a statistical model. The procedure can be described as follows:

1. The starting point is a collection of data. In this case: vibration data $\{\mathbf{y}_1, \mathbf{y}_2, \ldots, \mathbf{y}_N\}$ recorded by the LVDT sensors or accelerometers, and ground acceleration $\{\mathbf{a}_1, \mathbf{a}_2, \ldots, \mathbf{a}_N\}$ recorded at the base of the shaking table.
2. On the other hand, we choose a model to be fitted to the data. For the test structure, the model is the state space model (25)–(26).
3. Given the model and the data, we define the likelihood function.
4. Finally, the parameters of the model, $\theta = \{\mathbf{A}, \mathbf{B}, \mathbf{C}, \mathbf{Q}, \mathbf{R}\}$, are estimated at the maximum of the likelihood function.

The likelihood function for this model is computed using the innovations $\boldsymbol{\epsilon}_k$ (see Property A.1). Since $\mathbf{w}_k$ and $\mathbf{v}_k$ are Gaussian processes, the innovations also follow a Normal distribution:

$$\boldsymbol{\epsilon}_k \sim N(\mathbf{0}, \boldsymbol{\Sigma}_k). \tag{33}$$

Hence we may write the logarithm of the likelihood as:

$$\log L(\theta) = -\frac{1}{2} N n_y \log(2\pi) - \frac{1}{2}\sum_{k=1}^{N} \log|\boldsymbol{\Sigma}_k| - \frac{1}{2}\sum_{k=1}^{N} \boldsymbol{\epsilon}_k^T \boldsymbol{\Sigma}_k^{-1} \boldsymbol{\epsilon}_k. \tag{34}$$

where $\theta$ represents the vector of parameters. The estimation of these parameters is obtained at the maximum of Eqs. (34). The usual procedure is to choose a starting value for the parameters $\theta$ and then to use a numerical algorithm to find the maximum. In our opinion, the best option is the EM algorithm. This algorithm has been used to estimate the state space models (1)–(2) and (3)–(4) from vibration data, but we must derive the equations of the algorithm for the case of shaking table tests, that is, for the state space model given by (25)–(26). The details are shown in the following section.

### 3.2. The EM algorithm

#### 3.2.1. The joint log-likelihood function

The EM algorithm does not use the likelihood defined by Eq. (34). Instead, it uses the joint likelihood function assuming the states $\mathbf{x}_{1:N+1} = \{\mathbf{x}_1, \mathbf{x}_2, \ldots, \mathbf{x}_{N+1}\}$ are known in addition to the observations $\mathbf{y}_{1:N} = \{\mathbf{y}_1, \mathbf{y}_2, \ldots, \mathbf{y}_N\}$ and the ground accelerations $\mathbf{a}_{1:N} =$

$\{\mathbf{a}_1, \mathbf{a}_2, \dots, \mathbf{a}_N\}$. Both likelihoods reach the maximum at the same point, so in terms of estimates the solution is the same.

The joint likelihood function is:

$$\begin{aligned} L(\theta) &= p(\mathbf{x}_{1:N+1}, \mathbf{y}_{1:N} | \mathbf{a}_{1:N}, \theta) = p(\mathbf{x}_1, \mathbf{x}_2, \dots, \mathbf{x}_{N+1}, \mathbf{y}_1, \mathbf{y}_2, \dots, \mathbf{y}_N | \mathbf{a}_{1:N}, \theta) = \\ &= p(\mathbf{x}_1 | \mathbf{a}_{1:N}, \theta) \cdot p(\mathbf{x}_2, \mathbf{y}_1 | \mathbf{x}_1, \mathbf{a}_{1:N}, \theta) \cdot \\ &\quad p(\mathbf{x}_3, \mathbf{y}_2 | \mathbf{x}_1, \mathbf{x}_2, \mathbf{y}_1, \mathbf{a}_{1:N}, \theta) \cdot \dots \cdot p(\mathbf{x}_{N+1}, \mathbf{y}_N | \mathbf{x}_{1:N}, \mathbf{y}_{1:N-1}, \mathbf{a}_{1:N}, \theta) \\ &= p(\mathbf{x}_1 | \mathbf{a}_{1:N}, \theta) \cdot \prod_{k=1}^{N} p(\mathbf{x}_{k+1}, \mathbf{y}_k | \mathbf{x}_{1:k}, \mathbf{y}_{1:k-1}, \mathbf{a}_{1:N}, \theta) \end{aligned}$$

where $p(\cdot)$ denotes a generic density function. We take into account the following hypothesis:

- Model (25)–(26) verifies the Markov property:

  $$p(\mathbf{x}_{k+1}, \mathbf{y}_k | \mathbf{x}_{1:k}, \mathbf{y}_{1:k-1}, \mathbf{a}_{1:N}, \theta) = p(\mathbf{x}_{k+1}, \mathbf{y}_k | \mathbf{x}_k, \mathbf{a}_k, \theta).$$

  Therefore

  $$p(\mathbf{x}_{1:N+1}, \mathbf{y}_{1:N}, \mathbf{a}_{1:N}, \theta) = p(\mathbf{x}_1) \prod_{k=1}^{N} p(\mathbf{x}_{k+1}, \mathbf{y}_k | \mathbf{x}_k, \mathbf{a}_k, \theta). \tag{35}$$

- The noise terms $\mathbf{w}_k$ and $\mathbf{v}_k$ follow a Normal distribution:

  $$\begin{bmatrix} \mathbf{w}_k \\ \mathbf{v}_k \end{bmatrix} \sim N\left( \begin{bmatrix} \mathbf{0} \\ \mathbf{0} \end{bmatrix}, \begin{bmatrix} \mathbf{Q} & \mathbf{0} \\ \mathbf{0} & \mathbf{R} \end{bmatrix} \right). \tag{36}$$

  Then, $\mathbf{x}_{k+1}, \mathbf{y}_k | \mathbf{x}_k, \mathbf{a}_k, \theta$ will follow a Normal distribution as well,

  $$\mathbf{x}_{k+1}, \mathbf{y}_k | \mathbf{x}_k, \mathbf{a}_k, \theta \sim N\left( \begin{bmatrix} \mathbf{x}_{k+1} - \mathbf{A}\mathbf{x}_k - \mathbf{B}\mathbf{a}_k \\ \mathbf{y}_k - \mathbf{C}\mathbf{x}_k \end{bmatrix}, \begin{bmatrix} \mathbf{Q} & \mathbf{0} \\ \mathbf{0} & \mathbf{R} \end{bmatrix} \right). \tag{37}$$

  with probability density function:

  $$p(\mathbf{x}_{k+1}, \mathbf{y}_k | \mathbf{x}_k, \mathbf{a}_k, \theta) = p(\mathbf{x}_{k+1} | \mathbf{x}_k, \mathbf{a}_k, \theta) p(\mathbf{y}_k | \mathbf{x}_k, \mathbf{a}_k, \theta)$$

  $$p(\mathbf{x}_{k+1} | \mathbf{x}_k, \mathbf{a}_k, \theta) = \frac{1}{(2\pi)^{n/2} |\mathbf{Q}|^{1/2}} \exp\left( -\frac{1}{2} (\mathbf{x}_{k+1} - \mathbf{A}\mathbf{x}_k - \mathbf{B}\mathbf{a}_k)^T \mathbf{Q}^{-1} (\mathbf{x}_{k+1} - \mathbf{A}\mathbf{x}_k - \mathbf{B}\mathbf{a}_k) \right),$$

  $$p(\mathbf{y}_k | \mathbf{x}_k, \mathbf{a}_k, \theta) = \frac{1}{(2\pi)^{n_y/2} |\mathbf{R}|^{1/2}} \exp\left( -\frac{1}{2} (\mathbf{y}_k - \mathbf{C}\mathbf{x}_k)^T \mathbf{R}^{-1} (\mathbf{y}_k - \mathbf{C}\mathbf{x}_k) \right),$$

- The first state has Normal distribution, $\mathbf{x}_1 | \mathbf{a}_{1:N} \sim N(\mathbf{m}_1, \mathbf{P}_1)$:

  $$p(\mathbf{x}_1 | \mathbf{a}_{1:N}, \theta) = \frac{1}{(2\pi)^{n_x/2} |\mathbf{P}_1|^{1/2}} \exp\left( -\frac{1}{2} (\mathbf{x}_1 - \mathbf{m}_1)^T \mathbf{P}_1^{-1} (\mathbf{x}_1 - \mathbf{m}_1) \right).$$

In practice the log-likelihood is preferred because information is combined by addition and can be written as a sum of three uncoupled functions:

$$l(\theta) = \log L(\theta) = -\frac{1}{2} [l_1(\mathbf{m}_1, \mathbf{P}_1) + l_2(\mathbf{A}, \mathbf{B}, \mathbf{Q}) + l_3(\mathbf{C}, \mathbf{R})], \tag{38}$$

where, ignoring constants:

$$l_1(\mathbf{m}_1, \mathbf{P}_1) = \log |\mathbf{P}_1| + (\mathbf{x}_1 - \mathbf{m}_1)^T \mathbf{P}_1^{-1} (\mathbf{x}_1 - \mathbf{m}_1), \tag{39}$$

$$l_2(\mathbf{A}, \mathbf{B}, \mathbf{Q}) = N \log |\mathbf{Q}| + \sum_{k=1}^{N} (\mathbf{x}_{k+1} - \mathbf{A}\mathbf{x}_k - \mathbf{B}\mathbf{a}_k)^T \mathbf{Q}^{-1} (\mathbf{x}_{k+1} - \mathbf{A}\mathbf{x}_k - \mathbf{B}\mathbf{a}_k), \tag{40}$$

$$l_3(\mathbf{C}, \mathbf{R}) = N \log |\mathbf{R}| + \sum_{k=1}^{N} (\mathbf{y}_k - \mathbf{C}\mathbf{x}_k)^T \mathbf{R}^{-1} (\mathbf{y}_k - \mathbf{C}\mathbf{x}_k). \tag{41}$$

The problem with this likelihood is that the states are unknown variables. The EM algorithm proposes to work with the expected value of the likelihood because it can be computed using the Kalman filter output (this is called the Expectation or E step).

### 3.2.2. Expectation and maximization steps

The EM algorithm is an iterative method to maximize the likelihood. Each iteration of the EM algorithm consists of the following steps:

1. Assuming a value for the parameters, $\theta$, compute $\mathrm{E}[l(\theta) | \mathbf{y}_{1:N}, \mathbf{a}_{1:N}, \theta]$ (E-step, Property 3.1).
2. The M-step consists on maximizing $\mathrm{E}[l(\theta) | \mathbf{y}_{1:N}, \mathbf{a}_{1:N}, \theta]$ (M-step, Property 3.2).

**Property 3.1** (*E-step*). *Given the parameters of model (25)–(26), $\theta$, the measured data, $\mathbf{y}_{1:N} = \{\mathbf{y}_1, \mathbf{y}_2, \dots, \mathbf{y}_N\}$, and the measured base accelerations, $\mathbf{a}_{1:N} = \{\mathbf{a}_1, \mathbf{a}_2, \dots, \mathbf{a}_N\}$, the expected value of the likelihood (38) is given by*

$$\begin{aligned} &\mathrm{E}[l(\theta) | \mathbf{y}_{1:N}, \mathbf{a}_{1:N}, \theta] = \mathrm{E}[l_1(\mathbf{m}_1, \mathbf{P}_1) | \mathbf{y}_{1:N}, \mathbf{a}_{1:N}, \theta] \\ &+ \mathrm{E}[l_2(\mathbf{A}, \mathbf{B}, \mathbf{Q}) | \mathbf{y}_{1:N}, \mathbf{a}_{1:N}, \theta] + \mathrm{E}[l_3(\mathbf{C}, \mathbf{R}) | \mathbf{y}_{1:N}, \mathbf{a}_{1:N}, \theta], \end{aligned}$$

*with*

$$\mathrm{E}[l_1(\mathbf{m}_1, \mathbf{P}_1) | \mathbf{y}_{1:N}, \mathbf{a}_{1:N}, \theta] = \log |\mathbf{P}_1| + \mathrm{tr}\left( \mathbf{P}_1^{-1} \left[ \mathbf{P}_1^N + (\mathbf{x}_1^N - \mathbf{m}_1)(\mathbf{x}_1^N - \mathbf{m}_1)^T \right] \right), \tag{42}$$

$$\begin{aligned} \mathrm{E}[l_2(\mathbf{A}, \mathbf{B}, \mathbf{Q}) | \mathbf{y}_{1:N}, \mathbf{a}_{1:N}, \theta] = &N \log |\mathbf{Q}| + \mathrm{tr}\big( \mathbf{Q}^{-1} \big[ \mathbf{S}_{x_1 x_1} - \mathbf{S}_{x_1 x} \mathbf{A}^T - \mathbf{A}\mathbf{S}_{x x_1} - \mathbf{S}_{x_1 a} \mathbf{B}^T \\ &- \mathbf{B}\mathbf{S}_{a x_1} + \mathbf{A}\mathbf{S}_{xa} \mathbf{B}^T + \mathbf{B}\mathbf{S}_{ax} \mathbf{A}^T + \mathbf{A}\mathbf{S}_{xx} \mathbf{A}^T + \mathbf{B}\mathbf{S}_{aa} \mathbf{B}^T \big] \big), \end{aligned} \tag{43}$$

$$\mathrm{E}[l_3(\mathbf{C}, \mathbf{R}) | \mathbf{y}_{1:N}, \mathbf{a}_{1:N}, \theta] = N \log |\mathbf{R}| + \mathrm{tr}\left( \mathbf{R}^{-1} \left[ \mathbf{S}_{yy} - \mathbf{S}_{yx} \mathbf{C}^T - \mathbf{C}\mathbf{S}_{xy} + \mathbf{C}\mathbf{S}_{xx} \mathbf{C}^T \right] \right), \tag{44}$$

*where*

$$\mathbf{x}_k^N = \mathrm{E}(\mathbf{x}_k | \mathbf{y}_{1:N}, \mathbf{a}_{1:N}, \theta), \tag{45}$$

$$\mathbf{P}_k^N = \mathrm{Var}(\mathbf{x}_k | \mathbf{y}_{1:N}, \mathbf{a}_{1:N}, \theta), \tag{46}$$

$$\mathbf{P}_{k+1,k}^N = \mathrm{Cov}(\mathbf{x}_{k+1}, \mathbf{x}_k | \mathbf{y}_{1:N}, \mathbf{a}_{1:N}, \theta). \tag{47}$$

$$\mathbf{S}_{x_1 x_1} = \sum_{k=1}^{N} \left( \mathbf{P}_{k+1}^N + \mathbf{x}_{k+1}^N (\mathbf{x}_{k+1}^N)^T \right), \tag{48}$$

$$\mathbf{S}_{x_1 x} = \sum_{k=1}^{N} \left( \mathbf{P}_{k+1,k}^N + \mathbf{x}_{k+1}^N (\mathbf{x}_k^N)^T \right), \quad \mathbf{S}_{x x_1} = \mathbf{S}_{x_1 x}^T, \tag{49}$$

$$\mathbf{S}_{xx} = \sum_{k=1}^{N} \left( \mathbf{P}_k^N + \mathbf{x}_k^N (\mathbf{x}_k^N)^T \right), \tag{50}$$

$$\mathbf{S}_{yy} = \sum_{k=1}^{N} \left( \mathbf{y}_k \mathbf{y}_k^T \right), \tag{51}$$

$$\mathbf{S}_{yx} = \sum_{k=1}^{N} \left( \mathbf{y}_k (\mathbf{x}_k^N)^T \right), \quad \mathbf{S}_{xy} = \mathbf{S}_{yx}^T, \tag{52}$$

$$\mathbf{S}_{xa} = \sum_{k=1}^{N} \left( \mathbf{x}_k^N \mathbf{a}_k^T \right), \quad \mathbf{S}_{ax} = \mathbf{S}_{xa}^T, \tag{53}$$

$$\mathbf{S}_{x_1 a} = \sum_{k=1}^{N} \left( \mathbf{x}_{k+1}^N \mathbf{a}_k^T \right), \quad \mathbf{S}_{a x_1} = \mathbf{S}_{x_1 a}^T, \tag{54}$$

$$\mathbf{S}_{aa} = \sum_{k=1}^{N} \left( \mathbf{a}_k \mathbf{a}_k^T \right). \tag{55}$$

The conditional expectations $\mathbf{x}_k^N$, $\mathbf{P}_k^N$ and $\mathbf{P}_{k+1,k}^N$ are found using Properties A.1–A.3.

**Property 3.2** (*M-step*).

- *The maximum of* $\mathrm{E}[l_1(\mathbf{m}_1, \mathbf{P}_1) | \mathbf{y}_{1:N}, \mathbf{a}_{1:N}, \theta]$ *is attained at*

  $$\mathbf{m}_1 = \mathbf{x}_1^N, \tag{56}$$

  $$\mathbf{P}_1 = \mathbf{P}_1^N. \tag{57}$$

- *The maximum of* $\mathrm{E}[l_2(\mathbf{A}, \mathbf{B}, \mathbf{Q}) | \mathbf{y}_{1:N}, \mathbf{a}_{1:N}, \theta]$ *is attained at*

  $$\begin{bmatrix} \mathbf{A} & \mathbf{B} \end{bmatrix} = \begin{bmatrix} \mathbf{S}_{x_1 x} & \mathbf{S}_{x_1 a} \end{bmatrix} \begin{bmatrix} \mathbf{S}_{xx} & \mathbf{S}_{xa} \\ \mathbf{S}_{ax} & \mathbf{S}_{aa} \end{bmatrix}^{-1}, \tag{58}$$

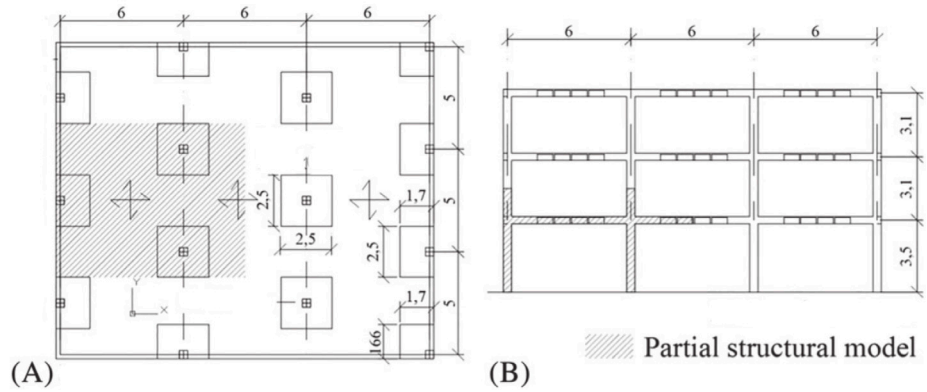


**Fig. 1.** Prototype structure: (A) plan; (B) elevation (dimensions in meters).

$$\mathbf{Q} = \frac{1}{N}\left(\mathbf{S}_{x_1x_1} - \mathbf{S}_{x_1x}\mathbf{A}^T - \mathbf{A}\mathbf{S}_{xx_1} - \mathbf{S}_{x_1a}\mathbf{B}^T - \mathbf{B}\mathbf{S}_{ax_1} + \mathbf{A}\mathbf{S}_{xa}\mathbf{B}^T + \mathbf{B}\mathbf{S}_{ax}\mathbf{A}^T + \mathbf{A}\mathbf{S}_{xx}\mathbf{A}^T + \mathbf{B}\mathbf{S}_{aa}\mathbf{B}^T\right). \quad (59)$$

- *The maximum of* $\mathrm{E}[l_3(\mathbf{C},\mathbf{R})|\mathbf{y}_{1:N},\mathbf{a}_{1:N},\theta]$ *is attained at*

$$\mathbf{C} = \mathbf{S}_{yx}\mathbf{S}_{xx}^{-1}, \quad (60)$$

$$\mathbf{R} = \frac{1}{N}\left(\mathbf{S}_{yy} - \mathbf{S}_{yx}\mathbf{C}^T - \mathbf{C}\mathbf{S}_{xy} + \mathbf{C}\mathbf{S}_{xx}\mathbf{C}^T\right). \quad (61)$$

The above equations can be obtained equating to zero the corresponding derivatives.

### 3.2.3. The proposed algorithm

The overall method can be summarized as an iterative procedure as follows:

1. Initialize the procedure by selecting starting values for the parameters

   $\theta_0 = \left(\mathbf{A}_0, \mathbf{B}_0, \mathbf{C}_0, \mathbf{D}_0, \mathbf{Q}_0, \mathbf{R}_0, \mathbf{m}_{1,0}, \mathbf{P}_{1,0}\right)$.

2. Run iterations for $j = 0, 1, 2, \ldots$:

   (a) Perform the E-Step.

   - Use Properties A.1, A.2 *y* A.3 to obtain the smoothed values $\mathbf{x}_k^N, \mathbf{P}_k^N$ and $\mathbf{P}_{k+1,k}^N$, for $k = 1, 2, \ldots, N$, taking into account $\theta_j$.
   - Calculate $\mathbf{S}_{x_1x_1}, \mathbf{S}_{x_1x}, \mathbf{S}_{xx}, \ldots, \mathbf{S}_{aa}$ according to (50)–(55).

   (b) Perform the M-Step.

   - Compute $\theta_{j+1}$ using (56)–(61).

3. Stop iterations when the value of the likelihood at step $j + 1$ differs from the likelihood at step $j$ by some predetermined, but small amount.

## 4. Application to shake table tests conducted on a reinforced concrete structure

The proposed algorithm was validated using the results of a dynamic seismic test performed with the shake table of the University of Granada. First, a prototype three-story RC waffle-flat-plate structure with an irregular column layout was designed according to the Spanish Concrete Code EHE-08 and the Spanish Seismic Code NCSE-02. Then, a portion of this structure was selected as shown in Fig. 1, and the test specimen was defined from this sub-structure by applying a scale factor of 2/5 for length. The rest of the physical quantities were scaled to satisfy similitude requirements. Therefore, the test specimen consists in a waffle-flat-plate structure sustained on an irregular column layout as can be seen in Figs. 2 and 3. The boundary conditions on the specimen were simulated by pinned joints at the zero moment locations and by introducing steel plates to reproduce the inertial forces induced by the mass of the upper levels, as can be seen in the 3D sketch of the experiment in Fig. 3. The added masses and the slab were instrumented with pairs of piezoelectric and seismic accelerometers that measured the absolute acceleration. Lasers and LVDTs measured the inter story relative displacements at each level. All sensors were calibrated against a control sensor and duplicated at each location to ensure no data was missed during the test. Fig. 4 shows the schematic geometry of the sub-assembly and the instrumentation employed in this paper. A more detailed description of the specimen geometry, material properties and sensor information can be found in [21].

The specimen was subjected to several bi-directional shake-table tests using the horizontal components of the accelerations registered at Calitri station during the Lucano-Campano earthquake (Italy, 1980). The ground motion recorded at Calitri station during the Lucano-Campano earthquake was selected because in the period range of interest (*i.e.* up to about 0.5 s), the geometric mean of the spectral accelerations of the NS and EW components of this earthquake are very close to the spectrum used in design (see Fig. 8). This is relevant to the tests because it ensures that the specimen is subjected to a seismic action that is similar and consistent with the seismic action used in the design.

For the purposes of this study, only the test with the lowest intensity in which the specimen remained elastic (undamaged) was used. The sampling frequency of the test was 600 Hz. However, since the response frequencies of interest are in the interval of 0 to 5 Hz, it was decided to filter the data with a 5th-order low-pass Butterworth filter with a cutoff frequency of 8 Hz.

During a shake table test there are multiple possible sources of noise such as cracking, pounding of cables, friction of set-up components, etc. These sources are difficult to identify or isolate; however, such noise sources typically have high frequencies which are far from the range of interest [0–8 Hz] and were filtered out with the low-pass Butterworth filter.

### 4.1. Modal parameters estimated using absolute accelerations as output data

Fig. 5 shows the input signal applied to the shaking table, that is, the components NS and EW of the Lucano-Campano earthquake registered at Calitri station. Fig. 6 shows the output absolute accelerations of the structure recorded by piezoelectric accelerometers located in the first story; four additional sensors were placed in the second story, with

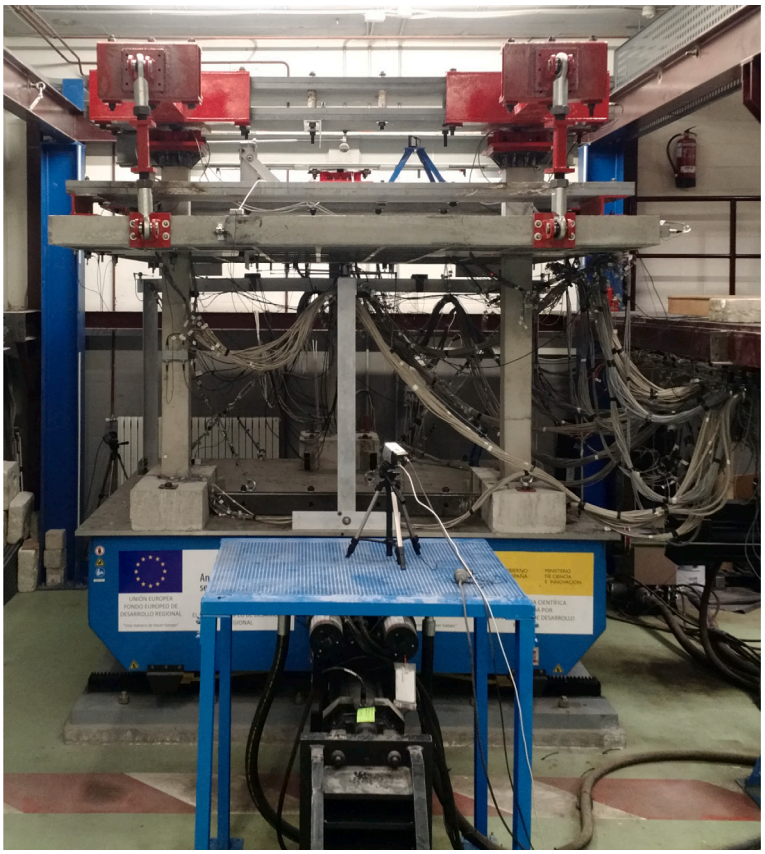

**Fig. 2.** General overview of the test specimen and the shake table.

**Fig. 3.** 3D Experimental set-up sketch.

positions similar than in the first story (see Fig. 4). In this section, the base accelerations applied to the shaking table (input data) and the absolute response accelerations (output data) measured by the piezoelectric accelerometers are used to estimate the modal parameters of the structure.

First, in order to have an initial idea of the vibration modes of the structure, the output-only frequency domain decomposition (FDD) method [22] was applied. The singular value spectra of the output data was computed and is shown with bold line in Fig. 7. This Figure plots the eigenvalues of the power spectral density (PSD) matrix computed at different frequencies. In the FDD method, the peaks of the singular value spectra are an estimation of the natural frequencies of the structure, and the eigenvectors of the PSD matrix are an estimation of the modal vectors. The FDD does not allow to obtain the damping ratios. From Fig. 7, three modes at frequencies 1.904, 2.343 and 2.636 Hz can be selected.

Then we applied the EM algorithm presented in Section 3.2.3. The first step is to select a starting point, $\theta_0 = (\mathbf{A}_0, \mathbf{B}_0, \mathbf{C}_0, \mathbf{Q}_0, \mathbf{R}_0)$. We cannot choose random values for these matrices because the algorithm will fail most of the times. On the other hand, like all the iterative

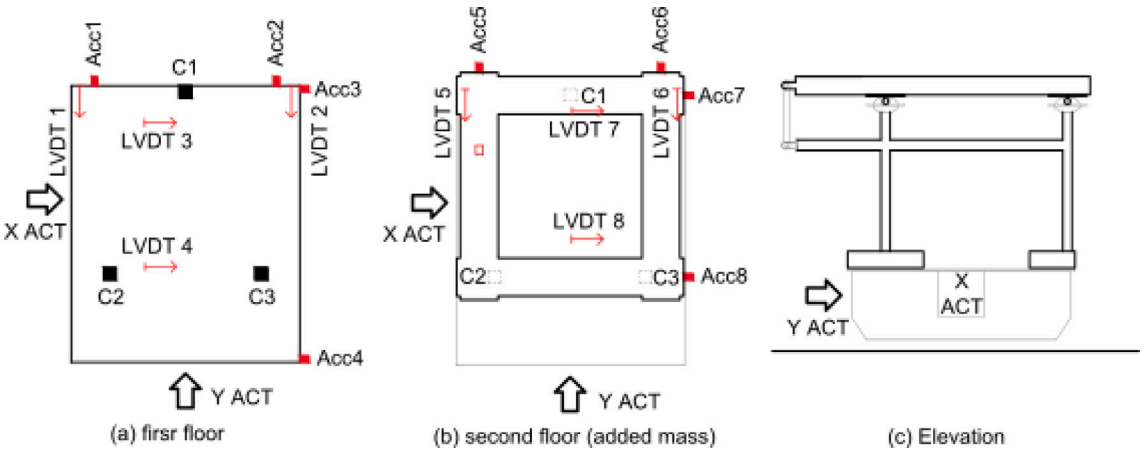


**Fig. 4.** Position of the sensors. EW and NS represent the two horizontal components of the earthquake.

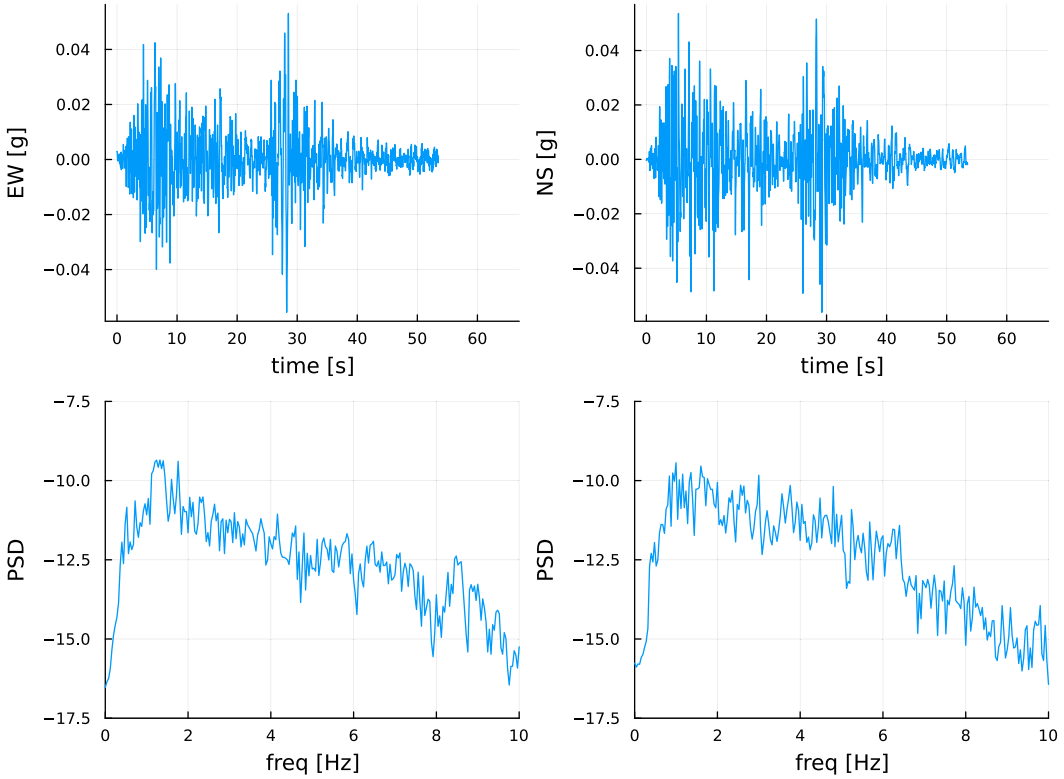


**Fig. 5.** Seismic accelerations recorded in the shaking table. The data is plotted in time and in frequency domain (logarithm of the Power Spectral Density function).

algorithms, the starting point must be close to the global maximum of the likelihood, because otherwise the algorithm will converge to a local maximum. Our approach is to use the Stochastic Subspace Identification (SSI) algorithm for output-only data [1]. Using this algorithm we estimated the model:

$$\mathbf{x}_{k+1} = \mathbf{A}_s\mathbf{x}_k + \mathbf{w}_k,\ \ \mathbf{w}_k \sim N(\mathbf{0}, \mathbf{Q}_s), \tag{62}$$

$$\mathbf{y}_k = \mathbf{C}_s\mathbf{x}_k + \mathbf{v}_k,\ \ \mathbf{v}_k \sim N(\mathbf{0}, \mathbf{R}_s). \tag{63}$$

The starting point was defined using this estimated model: $\mathbf{A}_0 = \mathbf{A}_s$, $\mathbf{C}_0 = \mathbf{C}_s$, $\mathbf{Q}_0 = \mathbf{Q}_s$, $\mathbf{R}_0 = \mathbf{R}_s$; $\mathbf{B}_0$ was equal to a matrix of zeros. Then we applied the proposed algorithm and the results are included in Table 1: the natural frequencies obtained with this method are: 2.015, 2.427 and 2.533 Hz. This table also includes the damping ratios and modal vectors corresponding to these frequencies.

### *4.2. Modal parameters estimated using relative displacements as output data*

In this section, the base accelerations applied to the base of the shaking table (input data) and the relative displacements (output data) measured by the LVDT are used to estimate the modal parameters of the structure. Fig. 9 shows the data recorded in the first story. Similarly to the accelerometers, four LVDT's sensors were placed in the first story and four additional LVDT's in the second story. According to the equations derived in Section 2, the displacement data used by the algorithm are relative displacements. The LVDT's in the first story measured the relative displacement between floor 1 and the shaking table, so these data verify the conditions of the algorithm. The LVDT's in the second floor measured the relative displacement between floor 2 and floor 1; therefore, the relative displacement to the shaking table is given by the sum of the displacement of floor 1 and floor 2. The input

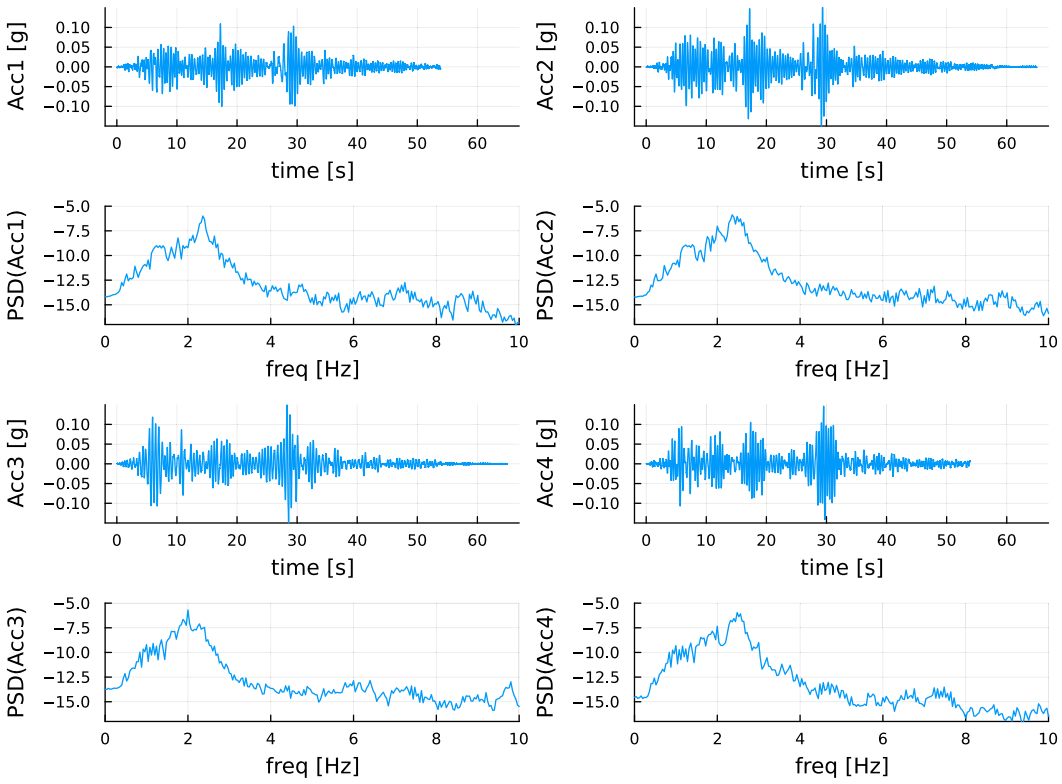


**Fig. 6.** Accelerations recorded by accelerometers 1, 2, 3 and 4. The data is plotted in time and in frequency domain.

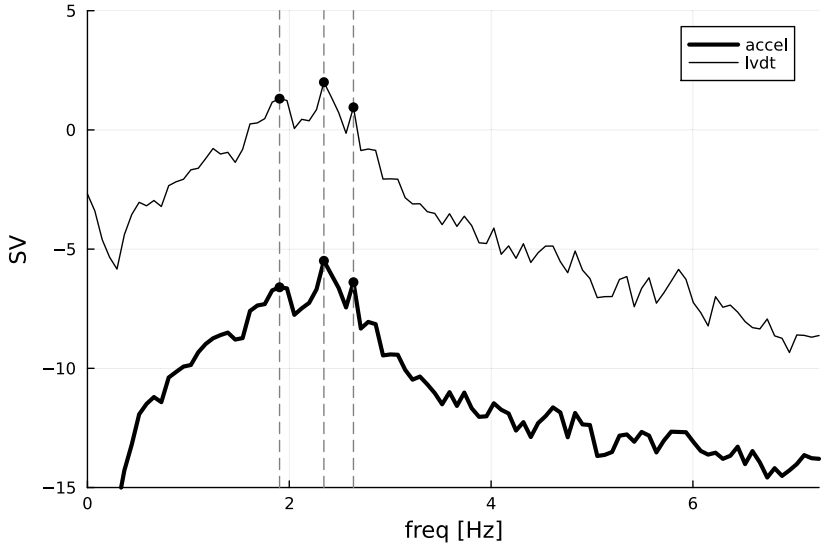


**Fig. 7.** Singular value spectra. Only the first eigenvalue is plotted.

signal is the same as in the previous section, that is, the acceleration shown in Fig. 5.

Similarly to Section 4.1, first the FDD method was applied to the relative displacements to get an initial idea of the vibration modes. The singular value spectra of the output data were computed and are shown with a thin line in Fig. 7. The frequencies obtained using the displacements (1.904, 2.343 and 2.636 Hz) are the same calculated from the absolute response accelerations.

Next, the EM algorithm proposed in Section 3 was applied using the SSI estimates as starting point. The frequencies, damping ratios and modal vectors obtained are summarized also in Table 1 and Fig. 10 depicts the shape of the vibration modes estimated from displacement data. Table 1 shows that the three frequencies obtained using the absolute response accelerations (Section 4.1) and the corresponding values calculated with the displacement data (Section 4.2) are almost identical.

The vibration modes were also compared with the MAC index:

$$MAC(\phi_1, \phi_2) = \frac{|\phi_1^T \phi_2|^2}{(\phi_1^T \phi_1)(\phi_2^T \phi_2)}, \tag{64}$$

which measures the similarity between the modal vectors $\phi_1$ and $\phi_2$: MAC index close to 1 means a high degree of similarity (the same modal vector), while MAC index near cero means orthogonal vectors. The results obtained with the shake table data are shown in Table 2.

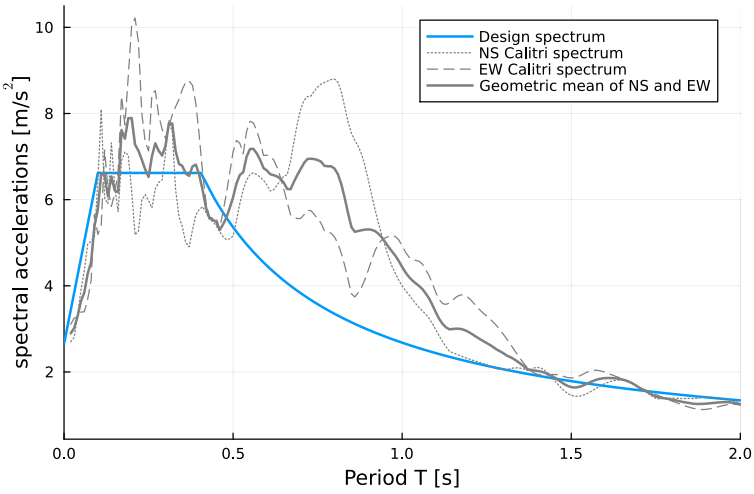


**Fig. 8.** Design spectrum versus Calitri response spectrum.

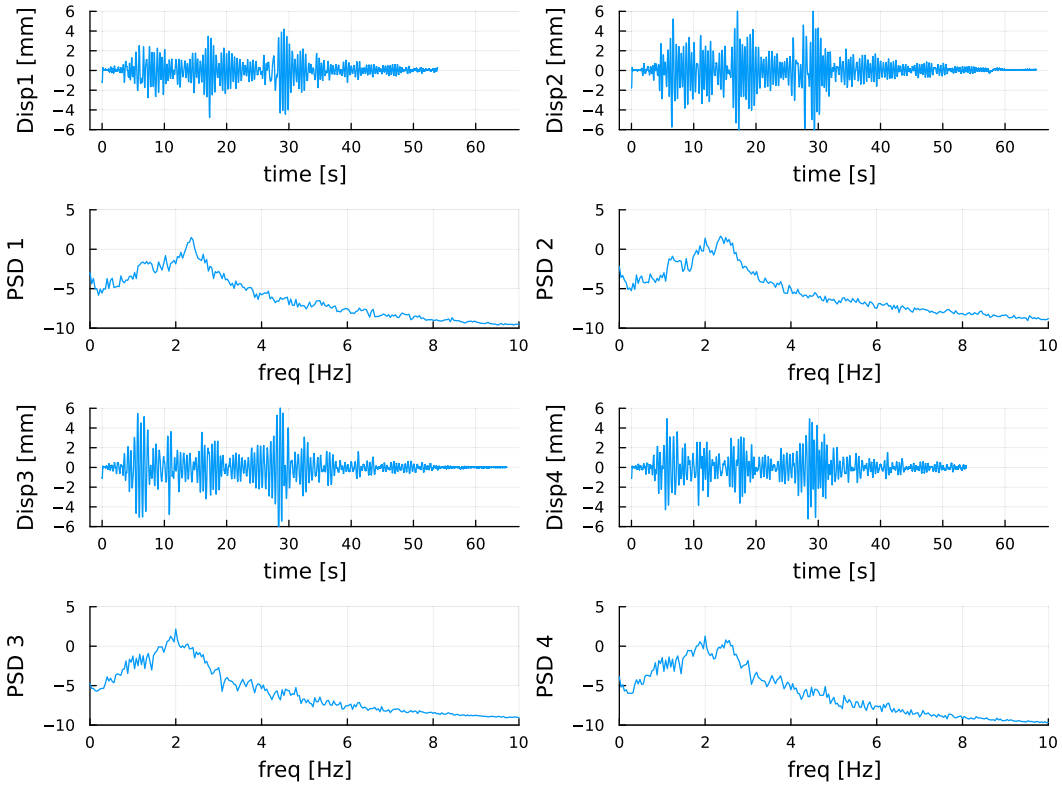


**Fig. 9.** Displacements recorded by LVDT's 1, 2, 3 and 4. The data is plotted in time and in frequency domain.

It can be seen that the modal vectors estimated with both types of output data are essentially the same (high MAC index). In our opinion, the observed differences are due to the acceleration and displacement sensors not being located at exactly the same positions, and not due to the proposed algorithm. In fact, in Section 5 we applied the method to simulated data and did not observe differences between the modal vectors estimated from the displacement and acceleration data.

## 5. Application to simulated data

In this section we used data obtained from a numerical model in order to better understand the performance of the proposed method. Let us consider a 3-dof spring–mass–damper system with (see Eq. (7)):

$$\mathbf{M} = \begin{bmatrix} 1 & 0 & 0 \\ 0 & 1 & 0 \\ 0 & 0 & 1 \end{bmatrix}, \quad \mathbf{G} = \begin{bmatrix} 0.7706 & -0.1657 & 0.0000 \\ -0.1657 & 0.9363 & -0.2486 \\ 0.0000 & -0.2486 & 1.1020 \end{bmatrix},$$

$$\mathbf{K} = \begin{bmatrix} 600 & -400 & 0 \\ -400 & 1000 & -600 \\ 0 & -600 & 1400 \end{bmatrix}, \quad \mathbf{J} = \begin{bmatrix} 1 \\ 1 \\ 1 \end{bmatrix},$$

and $\mathbf{a}(t)$ is the EW component of the Lucano-Campano earthquake (see Fig. 5). The modal parameters of this model are given in Table 3.

Using this model we obtained the total acceleration and the relative displacement of the system. Then, we added some measurement noise according to the rule $y_k = q_k + 0.15\sqrt{\text{var}(q_k)}e_k$, $e_k \sim N(0,1)$, where $q_k$ represents the acceleration or relative displacement of each degree

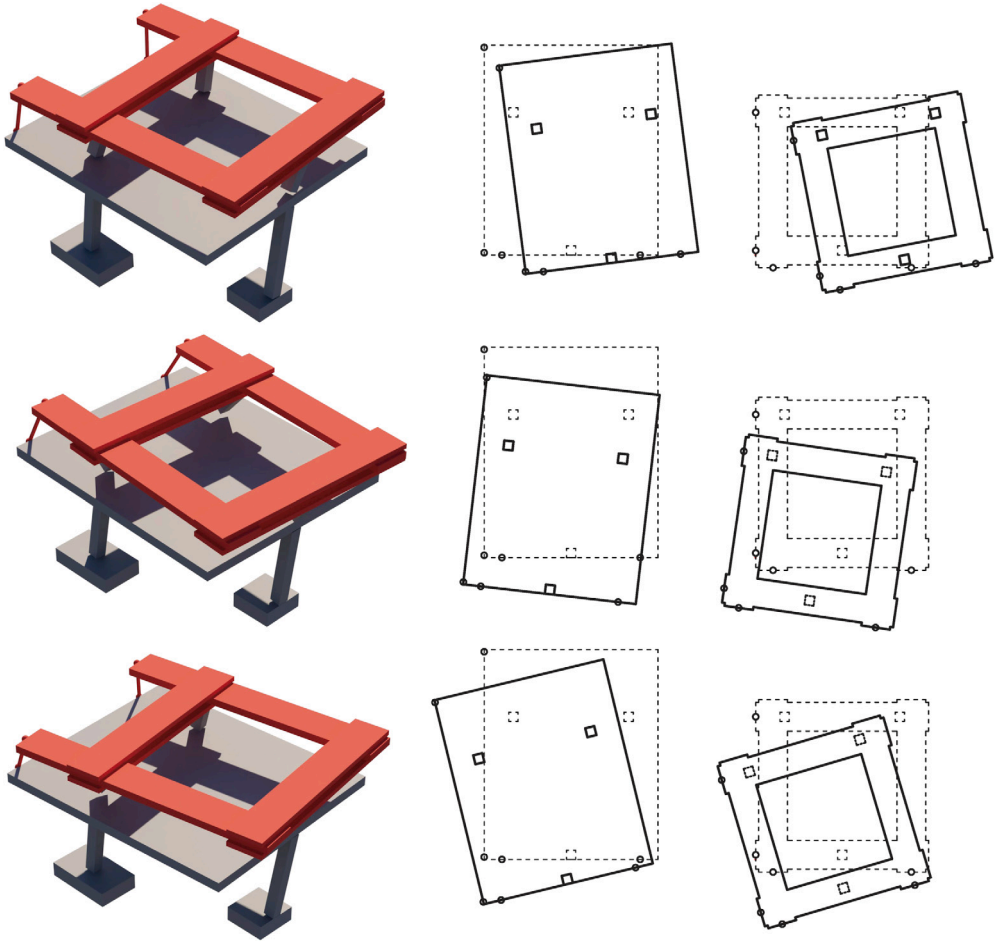

**Fig. 10.** Sketches of modal shapes.

**Table 1**
Modal parameters estimated using the proposed algorithm.

| | | | |
|---|---|---|---|
| EM from acceleration data | | | |
| $\hat{f}_i$ (Hz) | 2.0145 | 2.4274 | 2.533 |
| $\hat{\zeta}_i$ | 0.026 | 0.0156 | 0.023 |
| $\hat{\boldsymbol{\phi}}_i$ | −0.0123 | 0.4561 | −0.0414 |
| | −0.2383 | 0.3124 | −0.4303 |
| | −0.4864 | −0.2266 | −0.0139 |
| | −0.1245 | 0.0045 | 0.5227 |
| | 0.0177 | 0.5971 | −0.0843 |
| | −0.3444 | 0.4364 | −0.5626 |
| | −0.6793 | −0.3032 | 0.0139 |
| | −0.3326 | −0.0641 | 0.4646 |
| EM from displacement data | | | |
| $\hat{f}_i$ (Hz) | 2.0151 | 2.406 | 2.4956 |
| $\hat{\zeta}_i$ | 0.0374 | 0.0261 | 0.0444 |
| $\hat{\boldsymbol{\phi}}_i$ | 0.0213 | 0.5481 | −0.1021 |
| | −0.3259 | 0.1033 | −0.4926 |
| | −0.4355 | −0.1749 | 0.0980 |
| | −0.2510 | 0.1011 | 0.3429 |
| | 0.0746 | 0.7492 | −0.1684 |
| | −0.4741 | 0.1443 | −0.6486 |
| | −0.5514 | −0.2366 | 0.0974 |
| | −0.3260 | 0.0996 | 0.4014 |

of freedom at time instant $t_k = k(1/f_s)$, $f_s$ is the sampling frequency (600 Hz in this case).

We simulated 100 realizations of the system output using this procedure. Then, we estimated the modal parameters of the system using two methods: (1) the method proposed in this work, that is, the EM algorithm for the state space model given by Eqs. (25) and (25); (2) we also estimated the modal parameters using an OMA approach (state space model (1)–(2) and the SSI algorithm). The results are shown in Table 3.

**Table 2**
MAC values computed from modal vectors using accelerations (columns) and displacements (rows).

| $f(Hz)$ | 2.0145 | 2.4274 | 2.533 |
|---|---|---|---|
| 2.0151 | 0.9372 | 0.001 | 0.0133 |
| 2.406 | 0.0175 | 0.8065 | 0.0128 |
| 2.4956 | 0.0024 | 0.4356 | 0.9237 |

The main conclusions of this analysis are:

- The modal parameters obtained with the proposed method are more accurate than applying an OMA method. According to Table 3, the proposed method outperforms the SSI algorithm both in bias and variance.
- The results obtained using absolute acceleration data are similar to the results obtained using relative displacement data (in terms of the proposed algorithm).
- The natural frequencies are better estimated than the damping ratios. This fact is well known in the field of data-driven modal analysis and it is not exclusive of modal analysis using known base accelerations [1].

**Table 3**
Modal parameters estimated using the proposed EM algorithm and using an OMA method; *mean* stands for mean values, and *sd* stands for standard values.

| Modal parameters of the numerical model | | | |
|---|---|---|---|
| | Mode 1 | Mode 2 | Mode 3 |
| $\hat{f}_{real}$ (Hz) | 2.4762 | 4.7207 | 6.8973 |
| $\hat{\xi}_{real}$ (%) | 2.0000 | 1.4944 | 1.5000 |
| Results from absolute acceleration data | | | |
| mean[$\hat{f}_{em}$] (Hz) | 2.4810 | 4.7143 | 6.8804 |
| sd[$\hat{f}_{em}$] (Hz) | 0.0020 | 0.0015 | 0.0024 |
| mean[$\hat{f}_{oma}$] (Hz) | 2.3963 | 4.5959 | 6.6670 |
| sd[$\hat{f}_{oma}$] (Hz) | 0.0114 | 0.0052 | 0.0231 |
| mean[$\hat{\xi}_{em}$] (%) | 2.5946 | 1.5958 | 1.8896 |
| sd[$\hat{\xi}_{em}$] (%) | 0.0408 | 0.0107 | 0.0386 |
| mean[$\hat{\xi}_{oma}$] (%) | 1.6434 | 2.3192 | 2.5469 |
| sd[$\hat{\xi}_{oma}$] (%) | 1.2362 | 0.1156 | 0.2493 |
| mean[$MAC_{em}$] | 0.9999 | 0.9999 | 0.9999 |
| mean[$MAC_{oma}$] | 0.9925 | 0.9990 | 0.9626 |
| Results from relative displacement data | | | |
| mean[$\hat{f}_{em}$] (Hz) | 2.4779 | 4.7255 | 6.8999 |
| sd[$\hat{f}_{em}$] (Hz) | 0.0033 | 0.0027 | 0.0032 |
| mean[$\hat{f}_{oma}$] (Hz) | 2.3974 | 4.5985 | 5.1813 |
| sd[$\hat{f}_{oma}$] (Hz) | 0.0076 | 0.0608 | 3.0204 |
| mean[$\hat{\xi}_{em}$] (%) | 2.3214 | 1.7803 | 1.6441 |
| sd[$\hat{\xi}_{em}$] (%) | 0.0294 | 0.0224 | 0.0712 |
| mean[$\hat{\xi}_{oma}$] (%) | 1.7190 | 2.1383 | 4.0253 |
| sd[$\hat{\xi}_{oma}$] (%) | 0.6933 | 1.4920 | 3.9222 |
| mean[$MAC_{em}$] | 0.9999 | 0.9999 | 0.9957 |
| mean[$MAC_{oma}$] | 0.9994 | 0.9939 | 0.5542 |

- The MAC index calculated for estimated modal vectors (using the proposed algorithm) and real modal vectors are 0.999 (perfect estimation).
- We also applied the proposed method to absolute displacement data in order to study what happens when the hypotheses of the model are not fulfilled. Although this case is not included in Table 3, the results were not good: mode 3 is generally not estimated in almost all cases and the damping ratios estimated for modes 1 and 2 were wrong.

## 6. Conclusions and future research

This study investigated the application of input–output modal analysis and the maximum likelihood method to the particular case of structures which vibrations are originated by accelerations imposed at the base. The main conclusions are as follows:

- The model must be derived according to the problem: in this case, a state space model is derived taking into account that the system inputs are base accelerations. The use of state space models developed for EMA is not correct in this case, at least from a theoretical point of view.
- To estimate this model, we propose to use the Expectation–Maximization algorithm.
- The equations of the state space model of a structure excited through input accelerations applied at the base are formally identical regardless of the absolute response accelerations or the relative displacements being used as output data.
- If the absolute response accelerations and relative displacements measured during the vibration of the structure are consistent and correct, the frequencies and modal shapes obtained with both types of output data must be theoretically identical.
- Based on the previous conclusion, the comparison of the frequencies and modal shapes estimated independently using the absolute response accelerations or the relative displacements measured during tests, can be used to assess the reliability of the records provided by the instrumentation (*i.e.* accelerometers and LVDT's) in shaking table tests.
- The proposed state space model and algorithm was validated with the results of shaking table tests conducted on a RC structure and with simulated data. As expected, the frequencies and modal shapes estimated with the proposed state space model and algorithm were basically the same for absolute accelerations and relative displacements data.
- In the case of simulated data, it is shown that the proposed method gets better estimates than applying a traditional SSI algorithm for output-only data.

We include now a discussion about the limitations of the proposed method: the EM algorithm is an iterative algorithm, and like all the iterative algorithms, the final solution is highly sensible to the initial conditions. The usual way to deal with this problem is to choose a good starting point: in this work we propose to use the solution obtained with SSI for output-only data as starting point. We have seen in the section devoted to simulated data that the solution obtained with SSI-OMA is not always good, but it is good enough as a starting point for the EM algorithm. Another important drawback of the method is the time spent in the iterations: around 10 s in a normal laptop. It is not very time consuming, but it has to be taken into account.

For future research, we want to apply this method to other vibration data obtained in the shake table test. The data analyzed in this work are part of a bigger project in which the ground motion applied to the shake table was scaled in amplitude to 35%, 50%, 100%, 200%, and 300% of the ground motion recorded at Calitri station during the Campano Lucano earthquake (1980), in order to represent different levels of intensity. One of the objectives of the project was to study the different levels of damage to the structure according to the intensity of the earthquake. We have found that in the first three tests (35, 50 and 100%) the behavior of the structure was linear, and under the last two tests a non-linear response was observed. So the application of the proposed method in the case of nonlinear behavior is the next step in our research.

## CRediT authorship contribution statement

**Javier Cara:** Conceptualization, Formal Analysis, Methodology, Software, Visualization, Writing – original draft, Writing – review & editing . **David Escolano-Margarit:** Data curation, Formal Analysis, Visualization, Writing – original draft, Writing – review & editing, . **Amadeo Benavent-Climent:** Data curation, Writing – original draft, Writing – review & editing, Supervision, Funding acquisition.

## Declaration of competing interest

Nothing to declare.

## Acknowledgments

This work was supported by the Spanish Ministry of Science MCIN/AEI/10.13039/501100011033/[PID2020-120135RB-I00]; and FEDER (Fonds Européen de Dévelopment Régional).

## Appendix. Kalman filters and smoother

The following results are used in the Expectation step:

**Property A.1** (*The Kalman Filter*). *For the state space model specified in (25)–(26) with initial conditions* $x_1^0$ *and* $P_1^0$*, for* $k = 1, 2, \dots, N$,

$$\mathbf{x}_k^{k-1} = \mathbf{A}\mathbf{x}_{k-1}^{k-1} + \mathbf{B}\mathbf{a}_{k-1}, \tag{65}$$

$$\mathbf{P}_k^{k-1} = \mathbf{A}\mathbf{P}_{k-1}^{k-1}\mathbf{A}^T + \mathbf{Q}, \tag{66}$$

*with*

$$\mathbf{x}_k^k = \mathbf{x}_k^{k-1} + \mathbf{K}_k \boldsymbol{\epsilon}_k, \tag{67}$$

$$\mathbf{P}_k^k = (\mathbf{I} - \mathbf{K}_k\mathbf{C})\mathbf{P}_k^{k-1}, \tag{68}$$

*where*

$$\mathbf{K}_k = \mathbf{P}_k^{k-1}\mathbf{C}^T \boldsymbol{\Sigma}_k^{-1}, \tag{69}$$

$$\boldsymbol{\epsilon}_k = \mathbf{y}_k - \mathrm{E}\left[\mathbf{y}_k | \mathbf{y}_{1:k-1}, \mathbf{a}_{1:k-1}, \theta\right] = \mathbf{y}_k - \mathbf{C}\mathbf{x}_k^{k-1}, \tag{70}$$

$$\boldsymbol{\Sigma}_k = \mathrm{Var}(\boldsymbol{\epsilon}_k) = \mathrm{Var}[\mathbf{C}(\mathbf{x}_k - \mathbf{x}_k^{k-1}) + \mathbf{v}_t | \mathbf{y}_{1:k-1}, \mathbf{a}_{1:k-1}, \theta] = \mathbf{C}\mathbf{P}_k^{k-1}\mathbf{C}^T + \mathbf{R}. \tag{71}$$

$\mathbf{K}_k$ *is called the Kalman gain and* $\boldsymbol{\epsilon}_k$ *are the innovations.*

**Property A.2** (*The Kalman Smoother*)**.** *For the state space model specified in (25)–(26) with initial conditions* $\mathbf{x}_N^N$ *and* $\mathbf{P}_N^N$ *obtained via Property A.1, for* $k = N-1, N-2, \ldots, 1$,

$$\mathbf{x}_k^N = \mathbf{x}_k^k + \mathbf{J}_k\left(\mathbf{x}_{k+1}^N - \mathbf{x}_{k+1}^k\right), \tag{72}$$

$$\mathbf{P}_k^N = \mathbf{P}_k^k + \mathbf{J}_k\left(\mathbf{P}_{k+1}^N - \mathbf{P}_{k+1}^k\right)\mathbf{J}_k^T, \tag{73}$$

*where*

$$\mathbf{J}_k = \mathbf{P}_k^k\mathbf{A}^T\left(\mathbf{P}_{k+1}^k\right)^{-1}. \tag{74}$$

**Property A.3** (*The Lag-One Covariance Smoother*)**.** *For the state space model specified in (25)–(26) and* $\mathbf{J}_t$ *and* $\mathbf{P}_N^N$ *obtained from Properties A.1 and A.2, for* $k = N, N-1, \ldots, 2$

$$\mathbf{P}_{k+1,k}^N = \mathbf{P}_{k+1}^N\mathbf{J}_k^T. \tag{75}$$

## Data availability

Data will be made available on request.

## References


[1] Reynders E. System identification methods for (operational) modal analysis: Review and comparison. Arch Comput Methods Eng 2012;19:51–124.

[2] Magalhães Caetano E, Cunha A, Flamand O, Grillaud G. Ambient and free vibration tests of the Millau Viaduct: Evaluation of alternative processing strategies. Eng Struct 2012;45:372–84. http://dx.doi.org/10.1016/j.engstruct.2012.06.038.

[3] Reynders E, Degrauwe D, Roeck GD, Magalhaes F, Caetano E. Combined experimental-operational modal testing of footbridges. J Eng Mech (ASCE) 2010;136(6):687–96.

[4] Brownjohn J. Long-term monitoring of dynamic response of a tall building for performance evaluation and loading characterisation. In: Proceedings of the 1st international operational modal analysis conference, Copenhagen, Denmark, April 2005. 2005, p. 143–54.

[5] Darbre G, de Smet C, Kraemer C. Natural frequencies measured from ambient vibration response of the arch dam of Mauvoisin. Earthq Eng Struct Dyn 2000;29(5):577–86.

[6] Cara J. Modal identification of structures from input/output data using the expectation–maximization algorithm and uncertainty quantification by mean of the bootstrap. Struct Control Heal Monit 2019;26(1). http://dx.doi.org/10.1002/stc.2272.

[7] Maes K, Nimmen Van, Lourens E, Rezayat A, Guillaume P, De Roeck G, Lombaert G. Verification of joint input-state estimation for force identification by means of in situ measurements on a footbridge. Mech Syst Signal Process 2016;75:245–60. http://dx.doi.org/10.1016/j.ymssp.2015.12.017.

[8] Deckers K, Guillaume P, Lefeber D, De Roeck Guido, Reynders Edwin. Modal testing of bridges using low-weight pneumatic artificial muscle actuators. In: Proceedings of IMAC 26, the international modal analysis conference. 2008.

[9] Santiago Bertero, Pablo A Tarazaga, Rodrigo Sarlo. In situ seismic testing for experimental modal analysis of civil structures. Eng Struct 2022;270. http://dx.doi.org/10.1016/j.engstruct.2022.114773.

[10] Ikeda Y. Verification of system identification utilizing shaking table tests of a full-scale 4-story steel building. Earthq Eng Struct Dyn 2016;45(4):543–62.

[11] Prowell I, Elgamal A, Uang CM, Luco J. Enrique, Romanowitz H, Duggan E. Shake table testing and numerical simulation of a utility-scale wind turbine including operational effects. Wind Energy 2014;17(7):997–1016.

[12] Mendes N, Lourenço PB, Campos-Costa A. Shaking table testing of an existing masonry building: assessment and improvement of the seismic performance. Earthq Eng Struct Dyn 2014;43(2):247–66.

[13] Rainieri C, Gargaro D, Fabbrocino G, Maddaloni G, Di.Sarno L, Prota A, Manfredi G. Shaking table tests for the experimental verification of the effectiveness of an automated modal parameter monitoring system for existing bridges in seismic areas. Struct Control Heal Monit 2018;25(7):e2165.

[14] Ji X, Fenves GL, Kajiwara K, Nakashima M. Seismic damage detection of a full-scale shaking table test structure. J Struct Eng 2011;137(1):14–21.

[15] Vukobratović V, Yeow TZ, Kusunoki K. Floor acceleration demands in three RC buildings subjected to multiple excitations during shake table tests. Bull Earthq Eng 2021;19. http://dx.doi.org/10.1007/s10518-021-01181-2.

[16] Li X, Kurata M, Wang Y, Nakashima M. Estimating earthquake-induced displacement responses of building structures using time-varying model and limited acceleration data. J Struct Eng 2025;147. http://dx.doi.org/10.1061/(ASCE)ST.1943-541X.

[17] Fu H, Cao Y, Qu Z. Substructural shake table testing for nonstructural elements of various damage sensitivity in a fixed-base and a base-isolated building. Eng Struct 2024;321. http://dx.doi.org/10.1016/j.engstruct.2024.119017.

[18] Lehmann Erich L, George Casella. Theory of point estimation. Springer-Verlag; 1998, https://link.springer.com/book/10.1007/b98854.

[19] Clough RW, Penzien J. Dynamics of structures computers and structures. California: Inc. Berkeley; 2003.

[20] Cara J. Computing the modal mass from the state space model in combined experimental-operational modal analysis. J Sound Vib 2016;370:94–110. http://dx.doi.org/10.1016/j.jsv.2016.01.043.

[21] Benavent-Climent A, Galé-Lamuela D, Donaire-Avila J. Energy capacity and seismic performance of RC waffle-flat plate structures under two components of far-field ground motions: Shake table tests. Earthq Eng Struct Dyn 2019;48:949–69. http://dx.doi.org/10.1002/eqe.3161.

[22] Brincker R, Zhang2 L, Andersen P. Modal identification of output-only systems using frequency domain decomposition. Smart Mater Struct 10:441.